*geosciences*

MDPI

*Article*

# Rapid India–Asia Initial Collision Between 50 and 48 Ma Along the Western Margin of the Indian Plate: Detrital Zircon Provenance Evidence

**Muhammad Qasim [1,2,3,*], Junaid Ashraf [4,5,6], Lin Ding [2,3], Javed Iqbal Tanoli [4], Fulong Cai [2,3,*], Iftikhar Ahmed Abbasi [1] and Saif-Ur-Rehman Khan Jadoon [2,3]**

1 Department of Earth Sciences, College of Science, Sultan Qaboos University, Al-Khoud, Muscat 123, Oman; iftikhar@squ.edu.om
2 State Key Laboratory of Tibetan Plateau Earth System, Resources and Environment, Institute of Tibetan Plateau Research, Chinese Academy of Sciences, Beijing 100101, China; dinglin@itpcas.ac.cn (L.D.); saif@itpcas.ac.cn (S.-U.-R.K.J.)
3 University of Chinese Academy of Sciences, Beijing 100101, China
4 Department of Earth Sciences, COMSATS University Islamabad, Abbottabad Campus, Abbottabad 22010, Pakistan; junaidashrafawan@gmail.com (J.A.); javed_iqbal@cuiatd.edu.pk (J.I.T.)
5 Department of Geological Engineering, Ankara University, 0600 Ankara, Turkey
6 Earth Sciences Application and Research Center, Ankara University, 0600 Ankara, Turkey
* Correspondence: m.qasim@squ.edu.om or mqasimtanoli@gmail.com (M.Q.); flcai@itpcas.ac.cn (F.C.)

**Abstract:** Constraining the collision timing of India and Asia requires reliable information from the coeval geological record along the ~2400 km long collisional margin. This study provides insights into the India–Asia collision at the westernmost margin of the Indian Plate using combined U-Pb geochronological data and sandstone petrography. The study area is situated in the vicinity of Fort Munro, Pakistan, along the western margin of the Indian Plate, and consists of the Paleocene Dunghan Formation and Eocene Ghazij Formation. The U-Pb ages of detrital zircons from the Dunghan Formation are mainly clustered between ~453 and 1100 Ma with a second minor cluster between ~1600 and 2600 Ma. These ages suggest that the major source contributing to the Dunghan Formation was likely derived from basement rocks and the cover sequence exposed mainly in Tethyan Himalaya (TH), Lesser Himalaya (LH), and Higher Himalayan (HH). Petrographic results suggest that the quartz-rich samples from the Dunghan Formation are mineralogically mature and have likely experienced log-distance transportation, which is possible in the case of an already established and well-developed river system delivering the sediments from the Craton Interior provenance. Samples of the overlying Ghazij Formation show a major detrital zircon age clustered at ~272–600 Ma in the lower part of the formation, comparable to the TH. In the middle part, the major cluster is at ~400–1100 Ma, and a minor cluster at ~1600–2600 Ma similar to the age patterns of TH, LH, and HH. However, in the uppermost part of the Ghazij Formation, ages of <100 Ma are recorded along with 110–166 Ma, ~400–1100 Ma, and ~1600–2600 Ma clusters. The <100 Ma ages were mainly attributed to the northern source, which was the Kohistan-Ladakh arc (KLA). The ~110–166 Ma ages are possibly associated with the TH volcanic rocks, ophiolitic source, and Karakoram block (KB). The Paleozoic to Archean-aged zircons in the Ghazij Formation represent an Indian source. This contrasting provenance shift from India to Asia is also reflected in the sandstone petrography, where the sample KZ-09 is plotted in a dissected arc field. By combining the U-Pb ages of the detrital zircons with sandstone petrography, we attribute this provenance change to the Asia–India collision that caused the provenance shift from the southern (Indian Craton) provenance to the northern (KLA and KB) provenance. In view of the upper age limit of the Ghazij Formation, we suggest the onset of Asian–Indian collision along its western part occurred at ca. 50–48 Ma, which is younger than the collision ages reported from central and northwestern segments of the Indian plate margin with 70–59 Ma and 56 Ma, respectively.

check for updates

**Citation:** Qasim, M.; Ashraf, J.; Ding, L.; Tanoli, J.I.; Cai, F.; Ahmed Abbasi, I.; Jadoon, S.-U.-R.K. Rapid India–Asia Initial Collision Between 50 and 48 Ma Along the Western Margin of the Indian Plate: Detrital Zircon Provenance Evidence. *Geosciences* **2024**, *14*, 289. https://doi.org/10.3390/geosciences14110289

Academic Editors: Khin Zaw, Charles Makoundi and Ilias Lazos

Received: 11 September 2024
Revised: 17 October 2024
Accepted: 26 October 2024
Published: 29 October 2024

**Keywords:** India–Asia collision; western margin; Sulaiman fold-and-thrust belt; Cenozoic sequence belt; U-Pb geochronology; detrital zircons

## 1. Introduction

The Indian Plate has a tectonic drift starting at ~300 Ma when Pangea segregated [1,2]. During this displacement, the Indian Plate detached from the African Plate and traveled ~9000 km, leading to the closure of the Tethys Ocean and the formation of the younger Himalayas orogenic belt [3,4]. Several significant events were interpreted to be associated with this drift, such as the eruption of the Deccan flood basalt during the Cretaceous, which is regarded as hotspot volcanism [5]. Subsequently, the obduction of ophiolite over the northern Indian margin indicates the initial stage of the collision process [6], followed by the terminal India–Asia collision at 60–56 Ma [3,7–10]. The timing of the terminal India–Asia collision event is still debated. Multiple studies were carried out to constrain the timing of the India–Asia collision, which includes high-resolution sedimentology and stratigraphy, dating of high-pressure (HP) and ultrahigh-pressure (UHP) metamorphic rocks, detrital zircon U-Pb geochronology, paleomagnetic constraints, acceleration and deceleration of plate velocity, and the dating of arc magmatic records [3,7,8,11–17]. These studies provided an array of ages for the onset of continent-continent collision ranging between ~70 and ~34 Ma [7,8,18–20].

However, the determination of the onset of the collision is more complex. In the western Himalayas, where the Kohistan-Ladakh arc (KLA) is sandwiched between the Indian Plate and the Karakoram Block (part of the Asian Plate). This timing may represent the onset of the collision of India or Asia with various island arcs and/or microcontinents intervening between them and the final India–Asia collision occurring afterward [21–23]. The accretion of the KLA with India, predating the Asia–India collision is recognized widely [8,24]. However, a few studies also invoked the idea of a first accretion of KLA with Asia [21,25].

Similarly, the hypothesis of the Greater Indian Basin (GIB) has also been criticized for its existence south of the Main Central Thrust (MCT), contradicting the evidence of the suture zone [5]. However, recent studies support GIB existence north of the Main Mantle Thrust (MMT) instead of the MCT, with the possibility of closure before ~56 Ma [14]. These different scenarios in the western Himalayas created conflicts in constraining the timing and location of the initial India–Asia collision. As far as the initial collision timing is concerned, the stratigraphic record from the Himalayas provides varying information. The Cretaceous–Eocene sedimentary sequence in the Tethyan Himalaya is considered to be the northernmost exposure that documents the oldest ages of the initial India–Asia collision between 70 and 59 Ma [4,9,26]. The onset of collision in the western Himalayas has been constrained around ~56 Ma by studying the foreland basin sequence [3,8,14]. In contrast, similar studies from India, Tibet, Nepal, Bengal, and Indo-Burma ranges provided different ages for the initial India–Asia collision, which implies a diachronous onset of collision across the belt. In this study, we constrain the initial collision timing from the westernmost margin of the Indian Plate and compare our ages with similar sedimentary proxies to test the model of diachronous collision.

The general trend of the Himalayas changes from northwest-southeast in India to northeast-southwest in Pakistan (Figure 1A). The Sulaiman fold-and-thrust belt (SFB) is a broad curvilinear belt formed as a result of the oblique collision between India and Asia along the sinistral Chaman fault zone [27]. The structures formed in the SFB are mostly duplexes [28]. The propagation of the frontal fault southward delivered eroded sediments from the main collision zone into the active Sulaiman foredeep, which is reflected by the exposure of a 7-km-thick molasse sequence in the Sibi Basin [29]. The tectonic framework of the western Himalayas is an important component in addressing the timing of the India–Asia collision. The timing of the initial India–Asia collision in the western Himalayas

was at ~55 Ma [8]. The plate velocities, HP and UHP metamorphism, and detrital record support this age in the western Himalayan [13,14,22]. The initial collision age in the westernmost segment of the Himalayas is crucial because this can evaluate the model of the diachronous India–Asia collision. The oldest age reported from the western margin is 65 Ma, which is based on the thrusting of ophiolites over Paleocene sedimentary rocks [30]. Zhuang et al. [31] carried a research on a section located ~700–800 km in the south in the Sulaiman-Kirther belt using an integrated approach consisting of detrital zircon U-Pb age dating, fission track ages, and Nd-Sr isotopic signatures and constrained the collision timing around ~50 Ma. Our previously reported ages (56 and 55 Ma) from the northern sections and the age from Zhuang et al. [32] supported the idea that the Tethys started to close from the north toward the west. However, the ~50 Ma age might be older because the reported provenance shift is from Oligocene sediments.

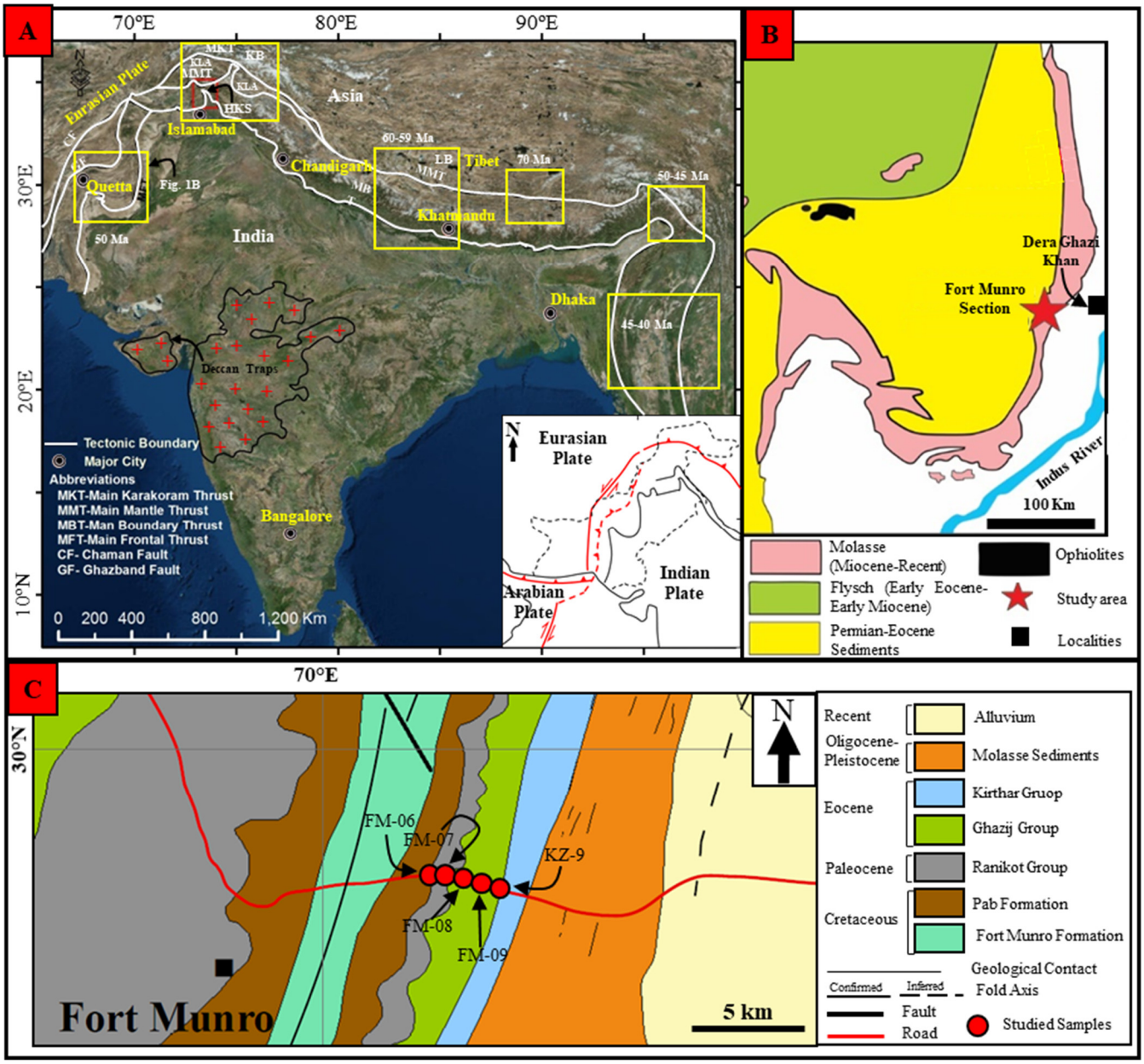


**Figure 1.** (**A**) The Google Earth satellite image showing major tectonic features. The initial India–Asia collision is marked for the particular sections represented by yellow boxes. The red black box indicates the western Himalayan syntaxial bend (Hazara-Kashmir Syntaxis; after Qasim et al. [14]).

(**B**) The simplified map showing the regional geology of the Sulaiman fold-thrust belt (SFB). Study area is marked with a red star (after Qasim et al. [33]). (**C**) Studied samples are marked on the geological map, which shows major stratigraphic units (after Jadoon and Zaib, [31]).

In order to provide better constraints on the initial collision, this study aims to investigate the Fort Munro section located in the SFB along the western margin of the Indian Plate (Figure 1A). The section is located in the southwestern part of SFB (Figure 1B,C). The selected section is more complete and continuous, where the horizon from where the provenance shift occurred can be traced. In this study, an advanced U-Pb detrital zircon dating is used, supplemented with sandstone petrography on the Cenozoic sequence to constrain the timing of the India–Asia initial collision. The U-Pb dating constrains the ages of the detrital zircons, which can be used to interpret the provenance by comparing the age patterns with the adjacent source regions [33,34].

## 2. Geological Setting and Stratigraphic Overview

The tectonics of the Pakistani Himalayas is mainly attributed to two main interactions. The first is in the northwest, driven by the India–Asia collision, while the second is in the south, where the Arabian, Indian, and Asian plates form a triple junction (Figure 1A inset). The Chaman Fault mainly controlled the first interaction in the western segment, while the Indus suture zone or Main Mantle Thrust (MMT) and Shyoke Suture Zone or Main Karakoram Thrust (MKT) pertained to the northern segment (Figure 1A) [6,35,36]. These faults separate the Indian Plate from the Afghan Block and the KLA from the Karakoram Plate, respectively (Figure 1). The southern interaction is mainly controlled by the Makran trench arc system, where the oceanic part of the Arabian plate subducts beneath the Afghan Block (Asian Plate) and the Chaman-Ornach Nal Fault System [37]. In response to these interactions, various fold-and-thrust belts formed throughout the Himalayas from east to west. On the western margin is the location of the SFB. The shape of the SFB suggests that the result of the rapid translation of the Indian plate in the southward direction is associated with weaker decollement of the tear fault-bounded thrust sheets. Magnetic stratigraphic dating indicates that the deformation pattern is younger in the foreland part [38]. In the SFB, the deformation pattern is gradually younger, reflected by the structural style, a noticeable topographic front, and seismicity recorded over the frontal folds [39]. Compared to other Himalayan fold-thrust belts, such as the Salt Range/Potwar plateau, which are connected to the main collision zone, the SFB is located along the transpression zone along the western boundary of the Indian Plate (Figure 1A). The initial collision in this belt is attributed to the Muslim Bagh Ophiolite emplacement during the Late Cretaceous to early Eocene [27].

The SFB is the widest of all Himalayan fold-and-thrust belts [27,28]. The SFB consisted of thick Triassic to Recent sedimentary rocks, which were deposited during pre-, syn- and post-collision. The Fort Munro Section is located at the southwestern margin of the SFB, where Cretaceous to Recent sedimentary rocks are exposed. The oldest units exposed in the study section are the Cretaceous Fort Munro and Pab formations, which are exposed in the core of an anticline (Figure 1C). The Fort Munro Formation consisted of mixed carbonate and clastic sequences. The carbonate consists mainly of thickly bedded limestone with minor interlayers of marl, shale, and sandstone [40]. The Pab Formation primarily consists of thick to massive sandstone (Figure 2A). The upper contact of the Pab Formation is unconformable with the overlying Ranikot Formation, which mainly comprises grey limestone, various colored sandstone, and shales. The Ranikot Formation is Paleocene in age [41]. It has an upper contact with the Dunghan Formation, which mainly consists of limestone with subordinate sandstone, shale, and marl (Figure 2B,C). The lower and upper contacts of the Dungan Formation with the Ranikot Formation and Ghazij group are conformable, respectively (Figure 1C). The age assigned to the Dunghan Formation is Late Paleocene (66–56 Ma) based on the reported foraminiferal assemblages [41]. The Ghazij Group mainly consisted of shale, limestone, and sandstone (Figure 2D). The shale is predominantly red and maroon (Figure 2E), occasionally purple. In comparison, sandstone

is red, grey, and green. The limestone is nodular and thin to thick-bedded (Figure 2E). The age of the Ghazij group is Eocene (55–48 Ma) based on the fossil assemblages [41].

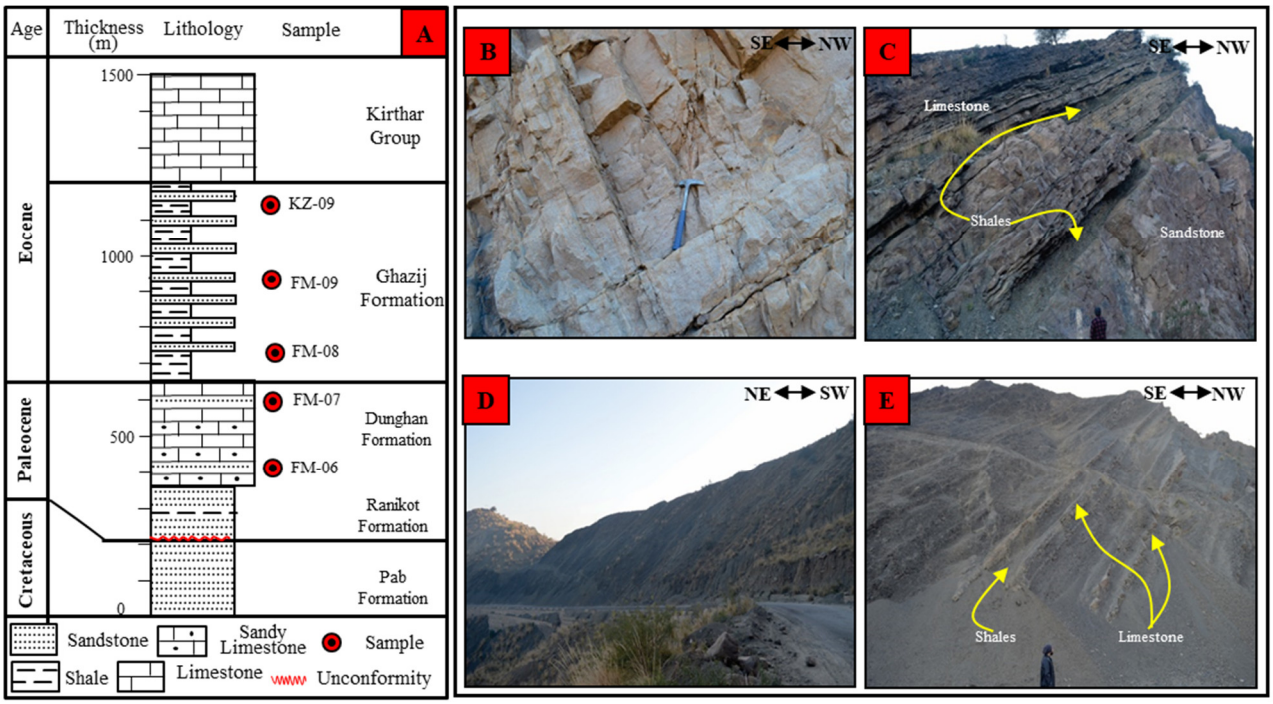


**Figure 2.** (**A**) Simplified lithological log of the studied section. (**B**–**E**) Key lithological variations in the studied formations are shown by field photographs taken along the main road. (**B**) Coarse sandstone of the Dunghan Formation. (**C**) Photograph of the Dunghan Formation shows limestone, shale, and sandstone units. (**D**) Shale interbedded with limestone and sandstone in the Ghazij Formation. (**E**) Close view of the outcrop showing shale and limestone interbeds of the Ghazij Formation.

## 3. Data and Methods

### *3.1. Petrography*

Sandstone petrography is a classical method used to study the composition and find out the provenance of the sandstones [42,43]. In this study, it is used as an aid to detrital zircon U-Pb geochronology. The five representative samples of the sandstones from the Fort Munro section were selected for petrographic observations. These samples were cut, and thin sections were prepared in the Rock Cutting and Thin section lab at the Department of Earth Sciences, COMSATS University Islamabad, Abbottabad Campus, Pakistan. The thin sections were observed under a polarizing petrographic microscope. Approximately 400 individual framework grains were counted from different views of the thin section using the point-counting method [42].

### *3.2. Zircon Imaging*

Zircon imaging depicts the internal structure of the individual detrital zircon grains. The detrital zircon grains were derived from various source regions containing metamorphic, igneous, and sedimentary rocks. The complex internal structure of the detrital zircons can lead to inaccurate age results if analyses were conducted on the transition zone. To avoid overlapping the analyzed spots on the core and rim of the detrital zircon, cathodoluminescence (CL) images (Supplementary Material Figure S1) were taken before the in situ U-Pb analyses. The U-Pb analysis spots were placed on the outer rim, where the internal structure is complex, to record the younger age of the zircons.

The zircon internal structure is important for differentiating between zircons from igneous and metamorphic origin [44]. The common zoning pattern observed in the imaged samples is oscillatory, which is a typical pattern of zircons derived from igneous origin [45]. The detrital zircons that experienced metamorphism reflect the core and rim structure. In our imaged zircons, a fair number of zircon grains exhibit core and rim structures. In the case of multiple metamorphic and magmatic events, the zircon internal structure becomes more complex, which is reflected by zoning structures comprising a xenocrystic core and sectoral pattern. Such zircon grains are also observed in the CL images. The zircon grains with a plane texture without any zoning are present too.

### 3.3. U-Pb Detrital Zircon Dating

One of the advanced and widely applied techniques in provenance studies is the U-Pb dating of the detrital zircons, which provides important and reliable information about the adjacent source regions [46]. A total of five samples were selected for U-Pb age dating: two from the Paleocene Dunghan Formation and three from the Eocene Ghazij Formation. Magnetic separation was applied to isolate the magnetic minerals from the crushed samples. These magnetic minerals were then further passed through different heavy liquids for the separation of detrital zircons. The zircon grains were mounted on double-sided adhesive tape, encased in epoxy resin within a closed circular mold, and then polished to create a flat surface of the mounted zircon grains. The polished zircon grains were washed with pure alcohol and diluted nitric acid to avoid lead contamination before in situ U-Pb analyses. The lab facility at the State Key Laboratory of Tibetan Plateau Earth System, Environment and Resources, Institute of Tibetan Plateau Research, Chinese Academy of Sciences, Beijing, China, was utilized for the U-Pb analyses.

One hundred detrital zircons from each sample were examined by Agilent 7500a Laser Ablation Inductively Coupled Plasma Mass Spectrometer (LA-ICP-MS). The two standard zircons were used to standardize the ages of the unknown detrital zircons. The standards used for the calibration were GJ-1 (weighted mean age of 609 Ma) [47] and 91500 (weighted mean age of 1065 Ma) [48]. The GJ-1 standard is used as the primary standard, while the 91500 standard was used as the secondary standard. The $^{207}Pb/^{206}Pb$ and $^{206}Pb/^{238}U$ age systems were used for zircons older and younger than 1000 Ma, respectively. Zircon grains with >10% discordance in either system were excluded from the final interpretation. Data reduction was performed using Glitter 4.0 software, and the final plots were created as probability density plots using Isoplot [49]. The U-Pb ages of the zircon grains are provided in Table S1 in Supplementary Material.

## 4. Results

### 4.1. Sandstone Petrography

#### 4.1.1. Dunghan Formation (~66–56 Ma)

The thin sections (FM-6 and FM-7) of the Dunghan Formation consist of 93–94% quartz, 3–5% feldspar, and 2–3% lithics (Table 1). The sample FM-6 represented the lower portion of the Dunghan Formation. Quartz grains are predominantly monocrystalline, though a few quartz grains with polycrystalline nature are present. The quartz grains exhibit undulatory extinction (3A). The feldspar includes both alkali and plagioclase varieties, while the lithics observed are of sedimentary origin, mostly carbonate (Figure 3A). The matrix consists of calcite. Accessory minerals such as muscovite and hematite are observed. The shape of the framework grains ranges from sub-angular to sub-rounded, with moderate to poor sorting (Table 2).

**Table 1.** Table shows the petrographic results for the samples of Dunghan and Ghazij formations. Q-Total quartz, Qp-Polycrystalline quartz, Qm-Monocrystalline quartz, F-total feldspar, Af-Alkali feldspar, Pf-Plagioclase feldspar, L-total lithics, Lm-Metamorphic lithics, Ls-Sedimentary lithics, Li-Igneous lithics, Bt-Biotite, Mus-Muscovite, Hm-Hematite and Cal.-Calcite.

| Sample No. | Quartz | | | Feldspar | | | Lithics (L) | | | Matrix/Cement | | Accessory Minerals (%) | | | Percentage Composition of Framework Grains | | | | | |
|---|---|---|---|---|---|---|---|---|---|---|---|---|---|---|---|---|---|---|---|---|
| | Qm | Qp | Q | Pf | Af | F | Ls | Lm | Li | Clay (%) | Cal. (%) | Bt | Mus | Hm | Q | F | L | Qm | F | L |
| FM6 | 292 | 8 | 300 | | | 16 | 6 | - | - | 8.8 | 9 | - | - | 2 | 93 | 5 | 2 | 93 | 5 | 2 |
| FM7 | 346 | 22 | 368 | 8 | 4 | 12 | 12 | - | - | - | - | - | 0.3 | 2 | 94 | 3 | 3 | 94 | 3 | 3 |
| FM8 | 308 | 16 | 324 | 1 | 3 | 4 | 8 | - | - | 7.5 | 8.3 | 0.3 | - | 2 | 96 | 1 | 3 | 96 | 1 | 3 |
| FM9 | 324 | 1 | 325 | - | 7 | 7 | 8 | - | - | 14 | - | - | 1 | 1.3 | 96 | 2 | 2 | 96 | 2 | 2 |
| KZ9 | 136 | - | 136 | - | 148 | 148 | 68 | - | - | - | 12 | - | - | - | 39 | 42 | 19 | 39 | 42 | 19 |

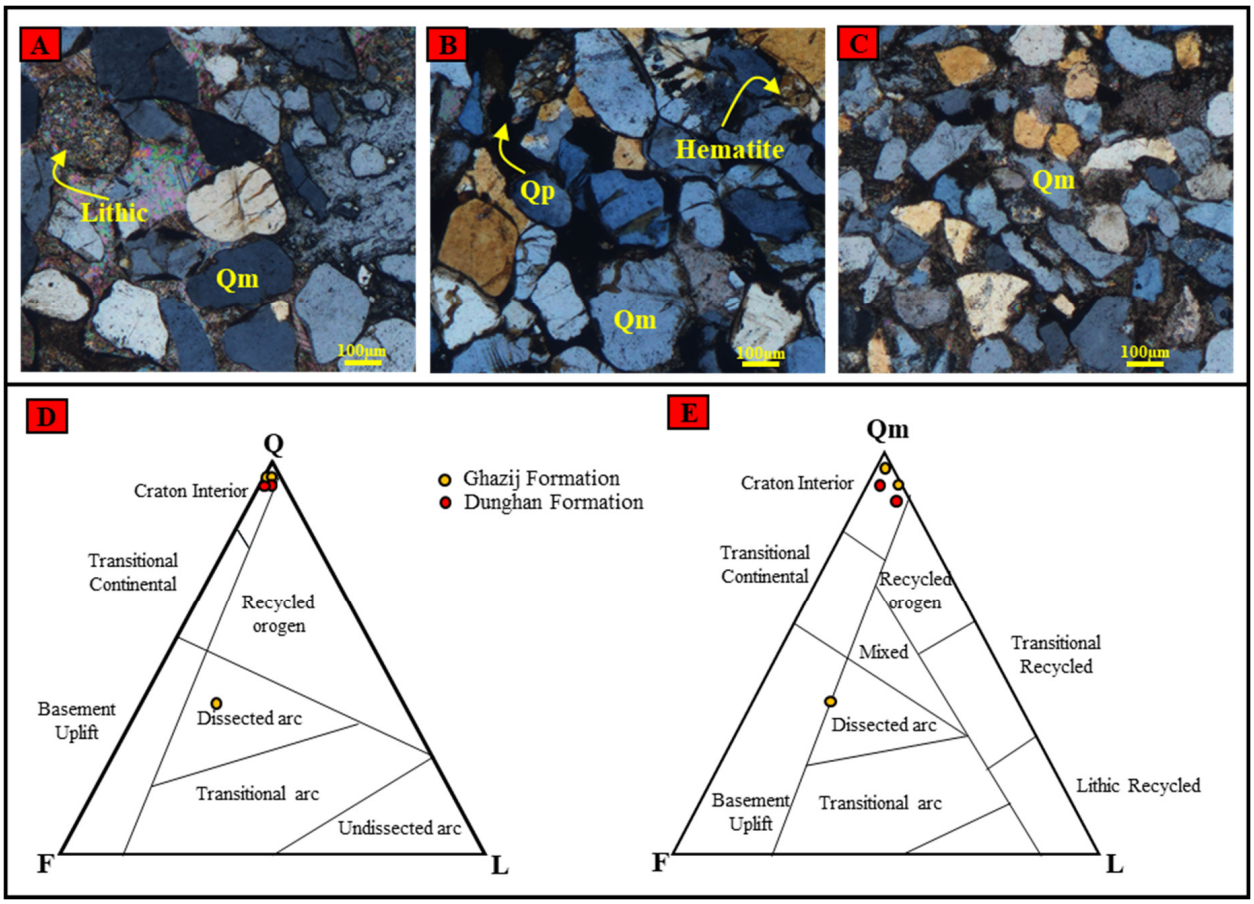


**Figure 3.** (**A**,**B**) Photomicrographs of the thin sections of the Dunghan Formation showing lithic fragments and monocrystalline quartz. (**C**) The photomicrograph of the Ghazij Formation shows polycrystalline quartz with hematite coating. (**D**,**E**) Ternary diagrams [42] show the tectonic provenance of Dunghan and Ghazij formations. Where Q represents total quartz, Qm represents monocrystalline quartz, F is used for total feldspar, and L stands for lithics.

**Table 2.** The petrographic data of the Dunghan and Ghazij formations show properties of the framework grains and other features.

| Formation Name | Sample No. | Grain Shape | | Fabric Support/ Contacts | Sorting | Maturity | |
|---|---|---|---|---|---|---|---|
| | | Roundness | Sphericity | | | Textural | Mineralogical |
| Dunghan Formation | FM6 | Sub-rounded | Low-Medium | Grain-supported, point contact | Moderate-Poor sorted | Sub mature | Mature |
| | FM7 | Subangular to Sub-rounded | Low-Medium | Grain-supported, pointed, concave-convex contacts | Moderate-Poor sorted | Mature | Mature |
| Ghazij Formation | FM8 | Sub-rounded to rounded | Low-Medium | Grain-supported, point contacts | Moderately sorted | Mature | Mature |
| | FM9 | Sub-rounded to rounded | Low-Medium | Matrix-supported, pointed contacts | Moderately sorted | Mature | Mature |
| | KZ9 | Sub-rounded to rounded | Medium-high | Grain-supported, pointed, concave-convex contacts | Moderately sorted | Immature | Mature |

#### 4.1.2. Ghazij Formation (~56–48 Ma)

The sample FM-8 represents the zone immediately above the basal contact with the Dungan Formation. The lowermost sample (FM-8) of the Ghazij Formation comprises 96% quartz, 1% feldspars, and 3% lithics (Table 1). Quartz grains are predominantly monocrystalline, with a few polycrystalline grains. The feldspar grains include both alkali and plagioclase varieties. The lithics are entirely sedimentary. Clay and calcite are observed in the matrix (Figure 3C). Accessory minerals such as biotite and muscovite are also present. The framework grains are sub-rounded to rounded, with moderate sorting (Table 2).

The thin section FM-9 of the Ghazij Formation, representing its middle zone, consists of 96% quartz, 2% feldspar, and 2% lithics (Table 1, Figure 3D,E). Most of the quartz grains are monocrystalline, with a few polycrystalline grains. The feldspar observed in this thin section is alkali feldspar. The lithics are sedimentary. No metamorphic and igneous lithics are observed. The matrix is clayey, and the accessory minerals include muscovite and hematite. The grains are sub-rounded to rounded, with moderate sorting (Table 2).

The third thin section (KZ-9) represented the zone immediately below the upper contact with the Kirthar Formation. The sample KZ-9 of the Ghazij Formation comprises quartz (39%), feldspar (42%), and lithics (19%). The quartz grains were mostly monocrystalline, and the feldspar grains were alkali feldspar. The observed lithics are sedimentary. The grains are sub-rounded to rounded in shape, with moderate sorting (Table 2).

### *4.2. U-Pb Zircon Geochronology*

#### 4.2.1. Dunghan Formation (66–56 Ma)

One hundred detrital zircon grains were analyzed from sample FM-6, which is representative of the lower part of the Dunghan Formation. One detrital zircon age was excluded due to >10% discordance. Ninety-nine concordant ages were obtained from this sample. The shape of zircon grains is mostly sub-rounded to rounded. Few zircon grains are euhedral (Supplementary Figure S1). The length of the zircon grains ranges between 50 and ~200 µm. One detrital zircon was excluded from the final ages due to >10% discordance in the age. The age spectrum of sample FM-6 reflects the major ages between ~486 and ~1102 Ma (~73%), with age peaks around ~518, ~588, ~729, ~871, and ~941 Ma

(Figure 4). The second age group ranges between ~1700 and ~2600 Ma, which is ~24% of the total detrital zircon ages. The major age peaks in this spectrum are at ~1753, ~1976, and ~2482 Ma (Figure 4). Few grains yielded ages between ~2800 and ~3250 Ma.

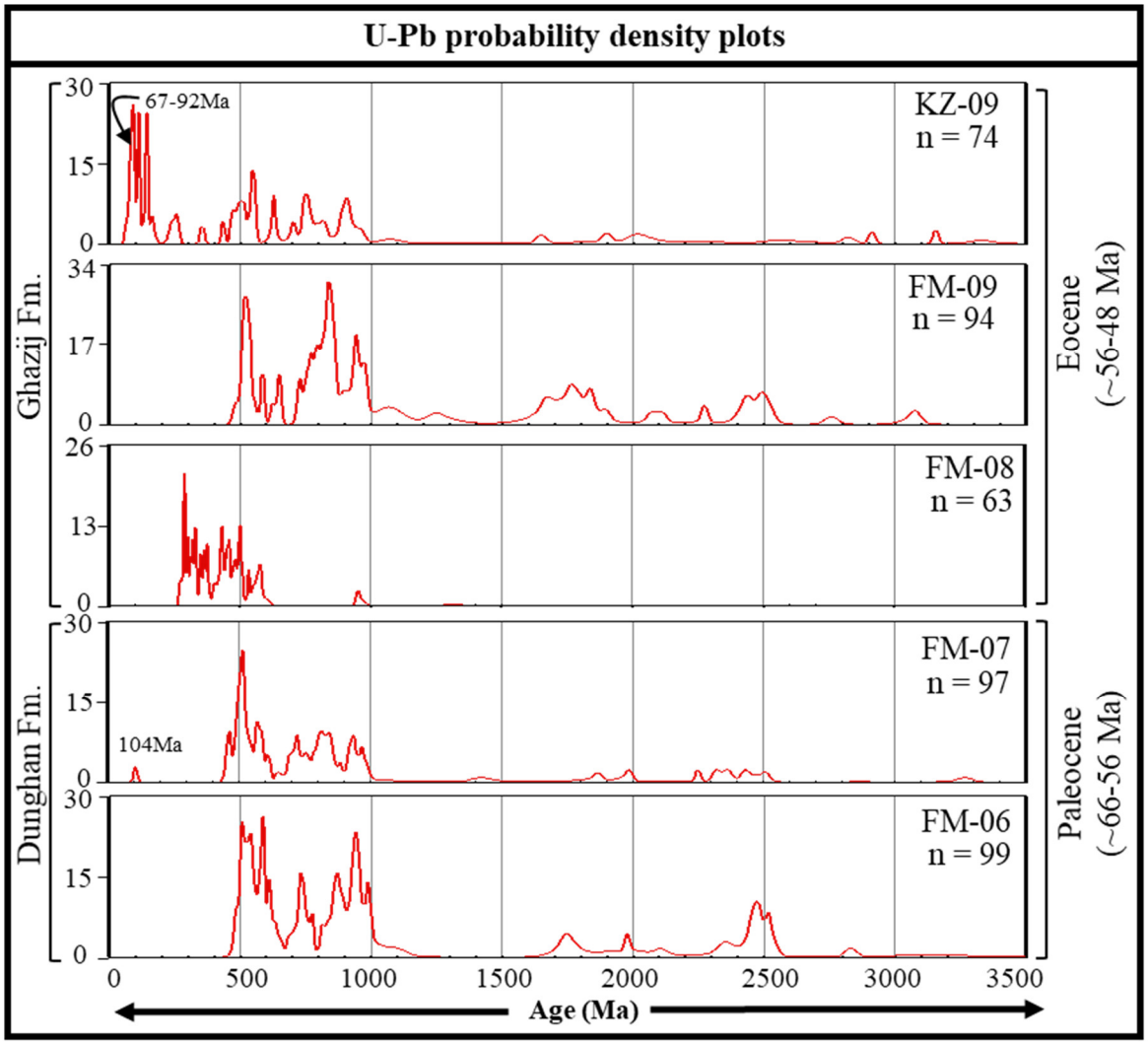


**Figure 4.** The U-Pb age data of the Dunghan and Ghazij formations are displayed as probability density plots (PDPs). The x-axis represents the age and the y-axis represents the number of zircon grains.

Sample FM-7 is representative of the upper zone of the Dunghan Formation and yields 97 usable concordant ages out of 100 analyses. The shape of the zircon grains varies from sub-rounded to rounded. A few zircon grains were elongated. Most of the zircon grains ranged in size between 50 and 150 µm (Supplementary Figure S1). Three detrital zircons were excluded due to >10% discordance in the obtained ages. The first major age cluster exists between ~453 and ~1000 Ma (Figure 4).

This broader age cluster is further subdivided into three sub-clusters, which are ~453–678 Ma with age peaks at ~500 and ~530 Ma, ~692–900 Ma with age peaks at ~750 and 820 Ma, and ~916–1000 Ma with age peak at ~940 Ma. The two minor age groups cluster at ~1800–2000 Ma and ~2200–2500 Ma (Figure 4). Few scattered Archean ages are measured. The youngest age documented in this sample is 104 Ma (Figure 4).

#### 4.2.2. Ghazij Formation (~56–48 Ma)

Three representative samples, FM-8, FM-9, and KZ-9, were collected from the Ghazij Formation, corresponding to the basal, middle, and upper stratigraphic levels of the formation, respectively. The detrital zircons in sample FM-8 are mostly rounded to sub-rounded with a diameter ranging between ~50 and ~100 µm. Few elongated grains are present, ranging in length between 50 and 200 µm. In addition, a few needle-like grains are present. The different zoning patterns are observed in the zircon grains. Some of the grains display a plain texture. However, grains with oscillatory zoning, sectoral zoning, and core-rim zoning are present. One hundred detrital zircons from sample FM-8 yielded 63 concordant ages. Thirty-seven detrital zircons are excluded from the final analyses due to age discordance >10%. The PDP displays the major age clusters at ~272–603 Ma with age peaks at ~280, ~310, ~440, and ~500 Ma. This age population is ~95% of the total detrital zircon ages. Three detrital zircon grains yield scattered ages at ~951, ~966, and ~1313 Ma (Figure 4).

The zircon grains in sample FM-9 are mainly rounded to sub-rounded with a diameter ranging between 50 and ~80 µm. The elongated and euhedral grains have a length of <100 µm. Only a few grains were long enough, with a length ranging between 100 and 200 µm. Most of the zircon grains show a plain texture. However, the sectoral and oscillatory zoning is also reflected by many grains (Supplementary Figure S1). One hundred zircon grains are selected for the U-Pb analyses and 94 concordant ages are obtained with <10% discordance. Six grains are excluded because they exhibit >10% discordance. The PDP reflects that the major age group exists between ~725 and ~1100 Ma, which is ~43% of the total detrital zircon ages. In this age group, the major age peaks are at ~836 and ~944 Ma (Figure 4). The second group ranges between ~482 and ~650 Ma with a peak age at ~524 Ma, which is ~18% of the total obtained ages. The third group of ages ranges between ~1600 and ~1900 Ma (Figure 4). This age range is ~17% of the total age population. About 10% of the detrital ages are clustered at ~2257–2511 Ma (Figure 4). Three scattered ages are reported between ~2700 and ~3100 Ma.

The sample KZ-9 represents the upper part of the Ghazij Formation. The detrital zircon grains are mainly rounded to sub-rounded with a diameter of >80 µm. Detrital grains with elongated shapes are also present, with a length ranging between ~50 and >100 µm. The round grains mainly display a plain texture. However, the elongated and euhedral grains show oscillatory and sectoral zoning patterns (Supplementary Figure S1). The zircon grains were smaller in size; therefore, 90 grains were selected in this sample for U-Pb analyses. Of these analyzed grains, the concordant ages are obtained from 74 grains. The rest of the detrital zircon grains reflect the ages with >10% discordance and, therefore, are excluded from the interpretation. The major age cluster is present between the ages of ~355 and ~1100 Ma, with age peaks at ~580 and ~760 Ma, which is ~46% of the total obtained ages. The second significant age cluster (~27%) is the younger age population, which is present between ~67 Ma and ~166 Ma (Figure 4). Three detrital grains yield Permian-Triassic ages. The rest of the detrital grains yield scattered ages between ~1600 and ~3350 Ma (Figure 4).

### *4.3. Th/U Ratio*

The Th/U of the zircon grains is used to distinguish between igneous and metamorphic zircons [50]. The Th/U ratio of the igneous zircons is usually >0.3, while in the case of metamorphic zircon, this ratio is <0.3 [45]. The Th/U ratio and detrital zircon U-Pb ages are displayed by a binary plot to discriminate the igneous and metamorphic zircons. The scattered plot shows that the major detrital zircons with ages of >500 Ma are likely derived from igneous rocks with fair contribution from metamorphic rocks (Figure 5). The Permian detrital zircons and their corresponding Th/U ratio suggest an igneous origin, which is more likely the Panjal Traps exposed in the lesser Himalayas. Similarly, the younger detrital zircons of <100 Ma portray a higher Th/U ratio (>0.3), which is plotted in the igneous field. This supports the derivation from the Kohistan-Ladakh Arc, which is an entirely igneous terrane.

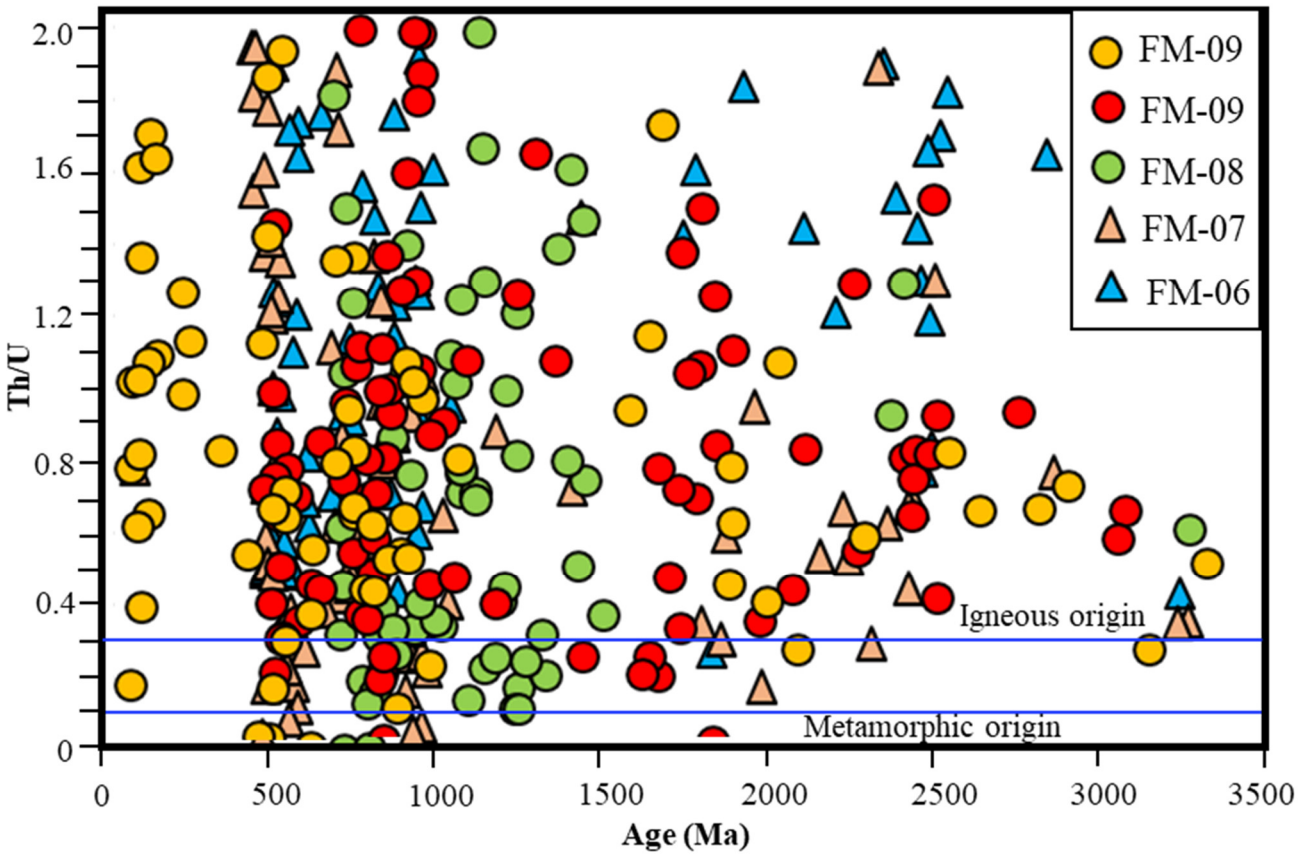


**Figure 5.** The two-dimensional binary plot displays the Th/U ratio and detrital zircons U-Pb ages. The Th/U ratio values above 0.3 represent igneous origin, while below 0.1 indicates metamorphic origin.

## 5. Discussion

### *5.1. U-Pb Ages and Source Terranes*

In the context of the India–Asia collision, the Karakoram Block (KB), Kohistan-Ladakh Arc (KLA), and Indian Plate were the possible source regions that could feed the evolving Himalayan foreland basin. The KB and KLA together represent the Asian source. At the same time, the Indian Plate sources consisted of rocks that are now part of the Lesser Himalaya (LH), Higher Himalaya (HH), and Tethys Himalaya (TH). The Asian and Indian source regions were located apart from each other before the India–Asia collision [51]. This separation is marked by the Tethys Ocean, which gradually closed as a result of the collision between the Asian and Indian plates. The mixing of these sources indicates the timing of the closure of the intervening ocean and the final India–Asia collision [8].

The zircon ages of the rocks of the KB are mainly clustered around ~18 to ~22 Ma, ~71 to 75 Ma, and ~103 to 110 Ma (Figure 6) [52]. The KLA age spectrum shows the major age range between ~40 and ~80 Ma [25]. Another population of the zircon ages are clustered between ~90 and ~110 Ma. The Indian craton sources yield zircon ages including the Archean and Proterozoic [53]. Metamorphic and sedimentary rocks are the major components of the Lesser Himalayan sequence (LHS), which has zircon isotopic ages between ~1700 and ~1900 Ma with a peak age at ~1880 Ma. In addition to this, a minor age group of the LHS existed between ~2500 and ~2600 Ma (Figure 6). The LHS sequence is deposited along the northern Indian margin and represents the southernmost source of the Paleo-Indian margin [54]. The age clusters of 700 to 1200 Ma, 1600 to 2000 Ma, and 2400 to 2600 Ma were common in the Precambrian sedimentary sequence exposed along the northern margin [55]. The HH was initially positioned with the LH and TH [51] or accreted later to the northern Indian margin during Gondwana orogenesis during the Cambrian-Early Ordovician [56]. Furthermore, the Higher Himalayan sequence (HHS) has zircon

ages ranging between ~900 and ~1100 Ma with minor age groups at ~500–650, ~1500–1800, and ~2400–2600 Ma. Similarly, the Tethyan Himalayan Sequence (THS) mainly comprises ages at ~480–570, ~700–1200, and ~2400–2700 Ma (Figure 6). The younger igneous rocks in the THS consisted of ages ranging between ~110 and ~140 Ma. Therefore, the pre-collision sequences received detritus mainly from the Indian provenance, including LHS, HHS, and THS. The first record of mixed provenance from the northern sources (Asian Source) indicates the onset of collision between India and Asia between 50 and 48 Ma.

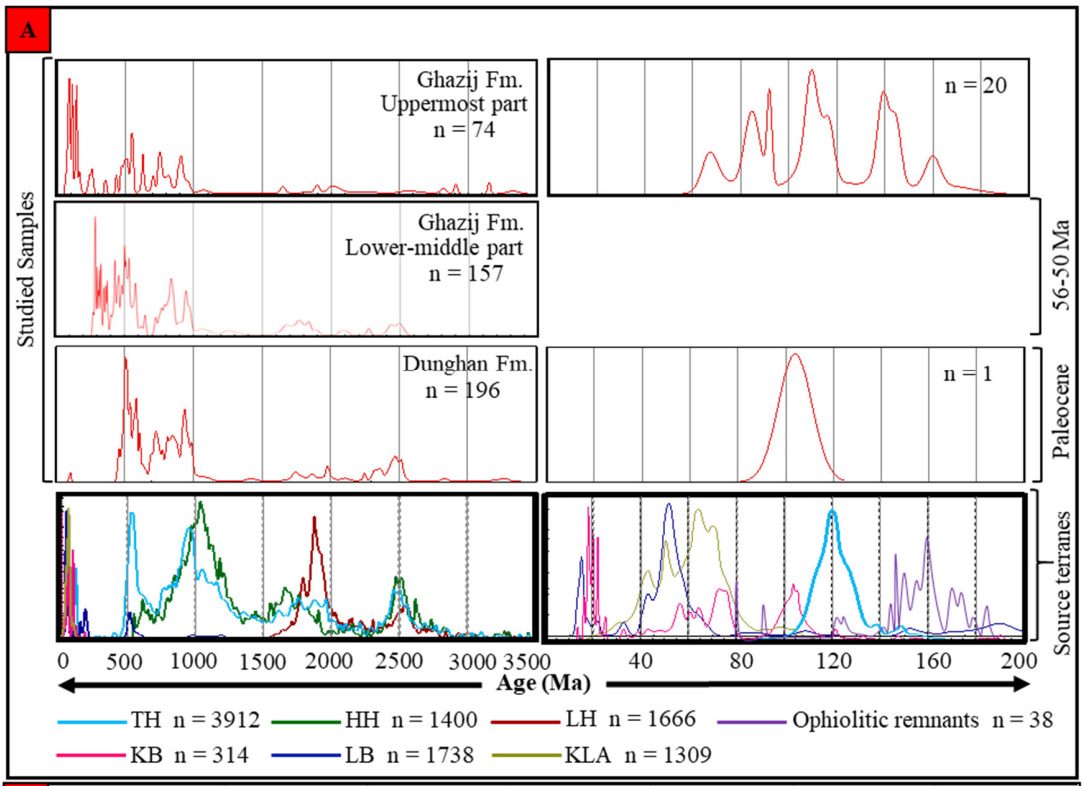


**B**

| | | TH | HH | LH | AS | Dunghan Fm. | Ghazij Fm. |
|---|---|---|---|---|---|---|---|
| Cross Correlation Coefficient | TH | 1.000 | 0.628 | 0.019 | 0.001 | 0.557 | 0.420 |
| | HH | | 1.000 | 0.001 | 0.007 | 0.112 | 0.038 |
| | LH | | | 1.000 | 0.006 | 0.005 | 0.012 |
| | AS | | | | 1.000 | 0.000 | 0.013 |
| | Dunghan Fm. | | | | | 1.000 | 0.827 |
| | Ghazij Fm. | | | | | | 1.000 |
| Likeness Value | TH | 1.000 | 0.809 | 0.261 | 0.294 | 0.704 | 0.674 |
| | HH | | 1.000 | 0.320 | 0.224 | 0.573 | 0.519 |
| | LH | | | 1.000 | 0.075 | 0.270 | 0.232 |
| | AS | | | | 1.000 | 0.255 | 0.321 |
| | Dunghan Fm. | | | | | 1.000 | 0.782 |
| | Ghazij Fm. | | | | | | 1.000 |
| Similarity Value | TH | 1.000 | 0.951 | 0.473 | 0.517 | 0.905 | 0.892 |
| | HH | | 1.000 | 0.539 | 0.446 | 0.813 | 0.775 |
| | LH | | | 1.000 | 0.220 | 0.486 | 0.458 |
| | AS | | | | 1.000 | 0.486 | 0.613 |
| | Dunghan Fm. | | | | | 1.000 | 0.924 |
| | Ghazij Fm. | | | | | | 1.000 |

**Figure 6.** (**A**) Comparison of the U-Pb ages of the Cenozoic sequence exposed in the Fort Munro section with the source terranes. (**B**) Quantitative analyses of the Cenozoic sequence with possible

source terranes. Values between 0 and 1 reflect a no-to-perfect relationship. The green to red color variation reflect perfect to no relationship.

### 5.2. Provenance of the Cenozoic Sequence

#### 5.2.1. Dunghan Formation

The samples FM-6 and FM-7 from the Paleocene Dunghan Formation show detrital zircon ages between ~453 and ~1100 Ma, which strongly matches with the TH ages (Figure 6A). The second group of ages exists between ~1600 and ~2600 Ma, which matches mutually with the TH, LH, and HH (Figure 6A). Furthermore, the younger 104 Ma detrital zircon ages may be derived from the TH volcanic rocks [7,57]. The contribution of these Indian-Plate sources is supported by the quantitative analyses carried out using DZ stats software 2.30 [58]. The values from 0 to 1 represent weak to perfect relationships, respectively. Data from the Dunghan Formation show a strong relationship with TH and HH reflected by values close to 1 (Figure 6B). All three statistical tests support this relationship. This is also evident by the highest percentage (~78%) of detrital ages between ~400 and 1100 Ma. The relationship with the LH is comparatively weaker, as reflected by values close to 0 (Figure 6B). The LH component typical of 1600 to 1900 Ma is also very low, which is ~8% of the total ages. This detrital age pattern of the Dunghan Formation suggests a mixed derivation from the TH, HH, and LH, representing Indian Provenance. The sandstone petrography of the samples FM-6 and FM-7 suggest the Craton Interior provenance. This craton interior provenance supports the detrital zircon provenance. This integrated provenance of the Dunghan Formation is part of the Indian Plate.

#### 5.2.2. Ghazij Formation

Three samples, FM-8, FM-9, and KZ-9, represent the bottom, middle, and top levels of the Eocene Ghazij Formation (Figures 1C and 2A). The lowermost samples yielded a major population of Carboniferous-Permian ages (~360–272 Ma). The Permian zircon grains could possibly be derived from the Panjal volcanics. These Panjal volcanics are exposed in LH. The second major population (~400–603 Ma) matched strongly with the TH. The composite pattern also yielded the major population between ~400–1100 Ma, which is strongly matched with the TH (Figure 6A). The statistical analyses also show a strong relationship with the TH and HH, as reflected by the values close to 1 (Figure 6B). In contrast, the presence of a minor age group between ~1600 Ma and 2600 Ma also suggests the contribution from LH and HH. The LH component is comparatively fair, as reflected by ~12% of the detrital zircon ages between 1600 Ma and 2000 Ma. The important presence of the younger detrital ages between ~67 Ma and ~110 Ma in the uppermost sample of the Ghazij Formation suggests the provenance shift (Figures 4 and 6A). This younger pattern indicates the contribution from KLA and KB, which are part of the Asian plate. The ages ~110–166 Ma may derive from TH volcanic rocks, ophiolitic sources, and KB. The provenance change from Indian to Asian sources is also reflected in the statistical analyses by the weak relationship between Dunghan and Ghazij formations. The sandstone petrography of the samples from the lower and middle parts suggests the craton interior provenance, whereas the uppermost sample shows dissected arc provenance. The integration of these results indicates that the lower to middle part of the Ghazij Formation may receive dominant detritus from Indian sources. In contrast, the uppermost part received detritus from both the Asian source and the Indian source. This suggests that the provenance shift occurred during the deposition of the upper part of the Ghazij Formation.

### 5.3. Implications for the Timing of India–Asia Collision

The India–Asia collision is constrained by marking the provenance shift, which is clearly reflected by the U-Pb age patterns of the detrital zircons. The Indian provenance is dominated by the zircons with ages >500 Ma, whereas the Asian provenance is characterized by the zircons with ages <150 Ma [3,4,8,14,31,59]. The integrated provenance of the Paleocene Dunghan Formation is mainly the Indian plate, which is evidenced by the pres-

ence of >500 Ma aged detrital zircons (Figure 6), where the major contribution is from the THS and some substantial contribution from LHS and HHS (Figure 6). This represents the contribution of the Indian provenance during the Paleocene (Figure 7). This provenance is also supported by the earlier study in the Kirther fold-belt located ~500 km to the southwest of the study area. The early–middle Paleocene samples from the Kirther fold-belt yielded similar detrital zircon age patterns dominated by >500 Ma ages [31]. Meanwhile, the lower and middle portions of the Eocene Ghazij Formation received the detritus mainly from the Indian plate. This provenance is reflected by the detrital zircons with ages >500 Ma. The samples show a broadly similar spectrum as of the Dunghan Formation (Figure 4). In contrast to the Dunghan Formation, a significant component of the Carboniferous–Permian age (~419–272 Ma) detrital zircons appeared in the basal sample of the Ghazij Formation. This component suggests the derivation mainly from the Permian Panjal volcanic and other associated rocks, which are exposed in the LH. This provenance is also primarily the Indian plate (Figure 6). However, the uppermost portion of the Ghazij Formation received the younger-aged detrital zircons (~67–110 Ma), which strongly resembled the KLA and KB (Figures 4 and 6). This arrival of the Asian detritus in the uppermost part of the Ghazij Formation marks the timing of the Tethys closure and India–Asia collision. The provenance shift in the Kirther belt is recorded in Oligocene–Pleistocene sediments, where <150 Ma detrital zircons become more prominent [31]. The double dating of the zircon grains using U-Pb and Fission Track (FT) dating in the earlier study provided supporting evidence in favor of the provenance shift and exhumation of the orogen [31]. Another prominent change in the Nd and Sr isotopic data is recorded by Roddaz et al. [60], where the εNd(0) value becomes −10 by ~50 Ma. This negative value was attributed to the collision.

Considering this supporting evidence, our interpretation strongly relates the appearance of young detrital zircons (<150 Ma) to the Asian source consisting mainly of the KLA with a small contribution from the Karakoram block. This change in the studied sample was recorded in the uppermost part of the Ghazij Formation. By relying on the upper age limit of the Ghazij Formation, it is suggested that the India–Asia collision occurred along the westernmost margin around ca. 50–48 Ma. The approximately 2400 km long Indian northern margin collided with the Asian margin diachronously. This diachronous collision is reflected by the previous studies extending from Pakistan in the west to the Indo-Burma ranges in the east. The timing of the collision reported in the eastern segment of the Himalayan mountain system in the Indo-Burma ranges is documented to be the earliest late Eocene [61], which is based on the provenance shift recorded by the appearance of Asian sediments. The studies in Tibet and Nepal, representing the central part of the Himalayan mountain system, reported collision ages ranging between ~70 Ma to 59 Ma [4,7,9–11,34,57]. Similarly, in the western segment of the Himalayan mountain system, the collision age reported from northern Pakistan is ~55 Ma [3,8,14,62]. Whereas, from the westernmost margin, the collision age reported by studying the sedimentary archive is ~50 Ma [31,60,63,64]. In the present study, our data recorded the first appearance of the Asian detritus within the uppermost part of the Ghazij Formation, which suggests the collision age to be ~50–48 Ma. Comparing the ages from the appearance of Asian detritus at different locations along the belt calls on the location of first contact of the Indian and Asian plates. The collision age is older in the central part of the Himalayas and becomes younger in the western and eastern margins. This pattern of the collision age suggested that the Indian plate collided with the Asian plate first in the central segment. Then, the intervening ocean closed gradually toward the west and east.

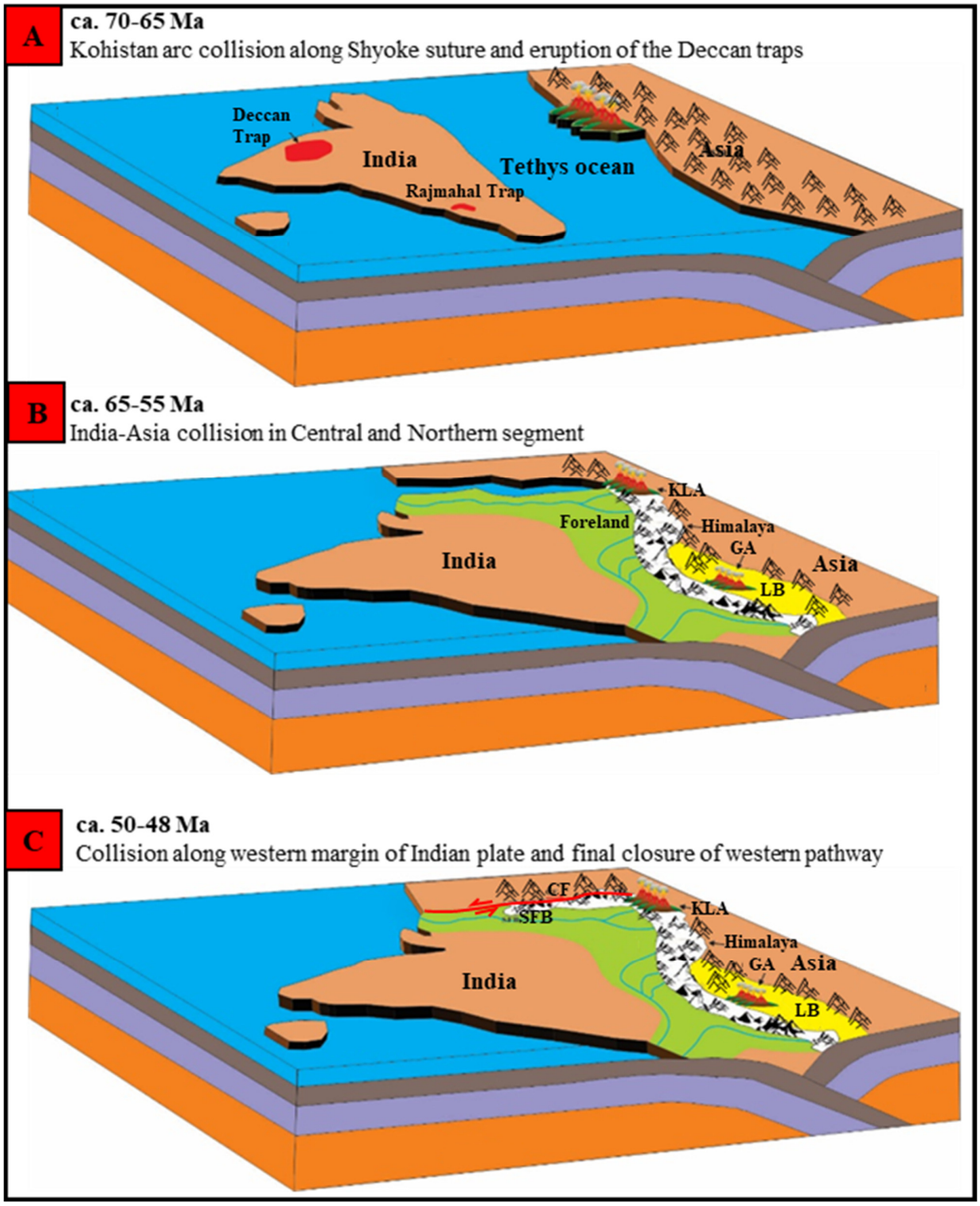


**Figure 7.** Tectonic model explaining the foreland basin evolution and collision scenario of the Indian plate since late Cretaceous to Eocene. (**A**) KLA and KB (Asian plate) collision during the late Cretaceous (70–65 Ma). At this time, the Deccan Traps erupted in the cratonic part of the Indian plate. The Asian margin is modified after Li et al. [65] and Zhang et al. [66]. (**B**) The initial collision of the Indian plate occurred in the central part to the west during the latest Cretaceous to Early Eocene and the Tethys Ocean closed in Central segments. (**C**) The final Tethys ocean closure occurred in the westernmost segment during the middle Eocene (50–48 Ma). GA-Gangdese arc, LB-Lhasa block, KLA-Kohistan-Ladakh Arc, SFB-Sulaiman Fold Belt, CF-Chaman strike-slip fault.

### 5.4. Tectonic Evolution

The India–Asia collision is measured as the first contact of continental plates after the vanishing of the oceanic lithosphere. Current research focuses on the Cenozoic succession of the Fort Munro Section, situated in the eastern Sulaiman fold-and-thrust belt. The rock formations studied in the Cenozoic sequence of the Fort Munro section comprise the Paleocene Dunghan Formation and the Eocene Ghazij Formation. The Paleocene Dunghan Formation mainly comprises marl, shale, and limestone, which were deposited in the marine environment [67]. The lower contact of the Dunghan Formation has been selected as a suitable datum, as the supply of the clastic sediments stopped to the basin and carbonate facies of the Dunghan Formation started to build. It is promising according to the surface and local dissimilarities in facies (from shallow nummulitic shoals to deeper marls and calc-turbidites) that it is not a consequence of a simple deepening event. Formerly, while interpreting this partitioning, the studies have associated it with the commencement of compressional tectonics ensued by the collision onset between the Asian and the Indian plates [24,68–70]. The U-Pb age pattern of the Dunghan Formation is matched well with the Himalayan source, thus reflecting the Indian provenance (Figure 7). The Eocene Ghazij Formation overlying the Dunghan Formation mainly comprises limestone, shale, and sandstone. The paleocurrent data reported from the Ghazij Formation suggested the southeastward flowing direction during the late Paleocene-early Eocene, which is northwestward during the late Cretaceous [71]. The provenance shift is recorded in the upper part of the Eocene Ghazij Formation by the appearance of <100 Ma detrital zircons, which is suggestive of the Asian source. This appearance marks the collision of India and Asia along the western margin.

## 6. Conclusions

This study resulted in the following conclusions.

1. The integrated provenance of the Paleocene Dunghan Formation suggests that the sediment input was mainly derived from the Indian source, as supported by the zircon age pattern consisting of ~453–1100 Ma and ~1600–2600 Ma, which are indicative of the TH, LH, and HH;
2. The samples of the Ghazij Formation representing the lower and middle parts consisted of the detrital zircons with ages clustered at ~272–300 Ma, ~400–1100 Ma, and ~1600–2600 Ma are similar to TH, HH, and LH, which also suggest the Indian provenance. However, the sample representing the uppermost part of the Ghazij Formation received the residue from the KLA, which is reflected by <100 Ma detrital zircons. This transition from Indian to Asian provenance occurred during the deposition of the upper part of the Ghazij Formation;
3. Relying on the sediment mixing of Indian and Asian affinity suggests the timing of the India–Asia collision occurred along the western margin by ca. 50–48 Ma, which is the age of the uppermost part of the Ghazij Formation;
4. Considering the proposed collision age, it can be concluded that the western margin of the Indian plate closed later than the northern and central segments.

**Supplementary Materials:** The following supporting information can be downloaded at https://www.mdpi.com/article/10.3390/geosciences14110289/s1: Table S1: The U-Pb age data of the studied samples. Figure S1: The CL images of the detrital zircons of the studied samples showing location of analyzed spots.

**Author Contributions:** M.Q.: Conceptualization, Investigation, Writing—Review and Editing, Project Administration, funding acquisition; J.A.: field data collection and MS thesis writing; L.D. and F.C.: Conceptualization, Investigation, Funding acquisition, Writing—Review and Editing; J.I.T.: Writing, review and editing; I.A.A.: Writing—Review and Editing. S.-U.-R.K.J.: Writing—original draft. All authors have read and agreed to the published version of the manuscript.

**Funding:** This work was financially supported by the Second Tibetan Plateau Scientific Expedition and Research Program (STEP; Grant No. 2019QZKK0708), Deanship Research Fund, Sultan Qaboos University, Oman (RF/SCI/ETHS/24/01), the Strategic Priority Research Program of the Chinese Academy of Sciences (XDA20070301), the National Natural Science Foundation of China BSCTPES project (Grant No. 41988101), and International Partnership Program of Chinese Academy of Sciences (131551KYSB20200021).

**Data Availability Statement:** The data that support the findings of the study are available in the article as a Supplementary File.

**Acknowledgments:** This is part of the PIFI postdoc research and an MS thesis at the Department of Earth Sciences, CUI, Abbottabad Campus, Pakistan. Andreas Scharf is thanked for his technical input and English editing.

**Conflicts of Interest:** The authors declare no conflict of interest.

## Abbreviations

HH: Higher Himalaya; TH: Tethyan Himalayan; LH: Lesser Himalaya; KB: Karakoram Block; LB: Lhasa Block; HP: High Pressure; UHP: Ultra-High Pressure; KLA: Kohistan-Ladakh arc; MMT: Main Mantle Thrust; MKT: Main Karakoram Thrust; MCT: Main Central Thrust; SFB: Sulaiman fold-thrust belt; Ma: Million years ago; CL: Cathode Luminescence; LAICPMS: Laser Ablation Inductively Coupled Plasma Mass Spectrometer

## References

1. Bortolotti, V.; Principi, G. Tethyan ophiolites and Pangea break-up. *Isl. Arc.* **2005**, *14*, 442–470. [CrossRef]
2. Chatterjee, S.; Goswami, A.; Scotese, C.R. The longest voyage: Tectonic, magmatic, and paleoclimatic evolution of the Indian plate during its northward flight from Gondwana to Asia. *Gondwana Res.* **2013**, *23*, 238–267. [CrossRef]
3. Awais, M.; Qasim, M.; Tanoli, J.I.; Ding, L.; Sattar, M.; Baig, M.S.; Pervaiz, S. Detrital Zircon Provenance of the Cenozoic Sequence, Kotli, Northwestern Himalaya, Pakistan; Implications for India–Asia Collision. *Minerals* **2021**, *11*, 1399. [CrossRef]
4. Ding, L.; Kapp, P.; Wan, X. Paleocene–Eocene record of ophiolite obduction and initial India-Asia collision, south central Tibet. *Tectonics* **2005**, *24*, TC3001. [CrossRef]
5. Garzanti, E.; Hu, X. Latest Cretaceous Himalayan tectonics: Obduction, collision or Deccan-related uplift? *Gondwana Res.* **2015**, *28*, 165–178. [CrossRef]
6. Searle, M.; Treloar, P. Was Late Cretaceous–Paleocene obduction of ophiolite complexes the primary cause of crustal thickening and regional metamorphism in the Pakistan Himalaya? *Geol. Soc. London Spec. Publ.* **2010**, *338*, 345–359. [CrossRef]
7. Cai, F.; Ding, L.; Yue, Y. Provenance analysis of upper Cretaceous strata in the Tethys Himalaya, southern Tibet: Implications for timing of India–Asia collision. *Earth Planet. Sci. Lett.* **2011**, *305*, 195–206. [CrossRef]
8. Ding, L.; Qasim, M.; Jadoon, I.A.K.; Khan, M.A.; Xu, Q.; Cai, F.; Wang, H.; Baral, U.; Yue, Y. The India–Asia collision in north Pakistan: Insight from the U–Pb detrital zircon provenance of Cenozoic foreland basin. *Earth Planet. Sci. Lett.* **2016**, *455*, 49–61. [CrossRef]
9. Hu, X.; Garzanti, E.; Moore, T.; Raffi, I. Direct stratigraphic dating of India-Asia collision onset at the Selandian (middle Paleocene, 59 ± 1 Ma). *Geology* **2015**, *43*, 859–862. [CrossRef]
10. Hu, X.; Wang, J.; An, W.; Garzanti, E.; Li, J. Constraining the timing of the India-Asia continental collision by the sedimentary record. *Sci. China Earth Sci.* **2017**, *60*, 603–625. [CrossRef]
11. Baral, U.; Lin, D.; Chamlagain, D.; Qasim, M.; Paudayal, K.N.; Neupane, B. Detrital zircon U–Pb ages, Hf isotopic constraints, and trace element analysis of Upper Cretaceous–Neogene sedimentary units in the Western Nepal Himalaya: Implications for provenance changes and India–Asia collision. *Geol. J.* **2019**, *54*, 120–132. [CrossRef]
12. DeCelles, P.; Kapp, P.; Gehrels, G.; Ding, L. Paleocene-Eocene foreland basin evolution in the Himalaya of southern Tibet and Nepal: Implications for the age of initial India-Asia collision. *Tectonics* **2014**, *33*, 824–849. [CrossRef]
13. Leech, M.L.; Singh, S.; Jain, A.; Klemperer, S.L.; Manickavasagam, R. The onset of India–Asia continental collision: Early, steep subduction required by the timing of UHP metamorphism in the western Himalaya. *Earth Planet. Sci. Lett.* **2005**, *234*, 83–97. [CrossRef]
14. Qasim, M.; Ding, L.; Khan, M.A.; Jadoon, I.A.K.; Haneef, M.; Baral, U.; Cai, F.; Wang, H.; Yue, Y. Tectonic Implications of Detrital Zircon Ages From Lesser Himalayan Mesozoic-Cenozoic Strata, Pakistan. *Geochem. Geophys. Geosystems* **2018**, *19*, 1636–1659. [CrossRef]
15. Wilke, F.D.; O'Brien, P.J.; Altenberger, U.; Konrad-Schmolke, M.; Khan, M.A. Multi-stage reaction history in different eclogite types from the Pakistan Himalaya and implications for exhumation processes. *Lithos* **2010**, *114*, 70–85. [CrossRef]

16. Jadoon, U.F.; Huang, B.; Shah, S.A.; Rahim, Y.; Khan, A.A.; Bibi, A. Multi-stage India-Asia collision: Paleomagnetic constraints from Hazara-Kashmir syntaxis in the western Himalaya. *GSA Bull.* **2021**, *134*, 1109–1128. [CrossRef]
17. Zhang, D.; Ding, L.; Chen, Y.; Schertl, H.-P.; Qasim, M.; Jadoon, U.K.; Wang, H.; Li, J.; Zhang, L.; Yue, Y.; et al. Two Contrasting Exhumation Scenarios of Deeply Subducted Continental Crust in North Pakistan. *Geochem. Geophys. Geosystems* **2022**, *23*, e2021GC010193. [CrossRef]
18. Huang, W.; Hinsbergen, D.J.; Lippert, P.C.; Guo, Z.; Dupont-Nivet, G. Paleomagnetic tests of tectonic reconstructions of the India-Asia collision zone. *Geophys. Res. Lett.* **2015**, *42*, 2642–2649. [CrossRef]
19. Lippert, P.; Van Hinsbergen, D.; Dupont-Nivet, G.; Kapp, P. Consensus on the Eocene Latitude of Lhasa and the Age of the Tethyan Himalaya-Asia Collision? In Proceedings of the AGU Fall Meeting Abstracts, San Francisco, CA, USA, 13–17 December 2010; p. 3.
20. Najman, Y.; Pringle, M.; Godin, L.; Oliver, G. Dating of the oldest continental sediments from the Himalayan foreland basin. *Nature* **2001**, *410*, 194–197. [CrossRef]
21. Khan, S.D.; Walker, D.J.; Hall, S.A.; Burke, K.C.; Shah, M.T.; Stockli, L. Did the Kohistan-Ladakh island arc collide first with India? *Geol. Soc. Am. Bull.* **2009**, *121*, 366–384. [CrossRef]
22. van Hinsbergen, D.J.; Steinberger, B.; Doubrovine, P.V.; Gassmöller, R. Acceleration and deceleration of India-Asia convergence since the Cretaceous: Roles of mantle plumes and continental collision. *J. Geophys. Res. Solid Earth* **2011**, *116*, B06101.
23. van Hinsbergen, D.J.J.; Lippert, P.C.; Li, S.; Huang, W.; Advokaat, E.L.; Spakman, W. Reconstructing Greater India: Paleogeographic, kinematic, and geodynamic perspectives. *Tectonophysics* **2019**, *760*, 69–94. [CrossRef]
24. Searle, M.; Khan, M.A.; Fraser, J.; Gough, S.; Jan, M.Q. The tectonic evolution of the Kohistan-Karakoram collision belt along the Karakoram Highway transect, north Pakistan. *Tectonics* **1999**, *18*, 929–949. [CrossRef]
25. Bouilhol, P.; Jagoutz, O.; Hanchar, J.M.; Dudas, F.O. Dating the India–Eurasia collision through arc magmatic records. *Earth Planet. Sci. Lett.* **2013**, *366*, 163–175. [CrossRef]
26. An, W.; Hu, X.; Garzanti, E.; Wang, J.-G.; Liu, Q. New Precise Dating of the India-Asia Collision in the Tibetan Himalaya at 61 Ma. *Geophys. Res. Lett.* **2021**, *48*, e2020GL090641. [CrossRef]
27. Jadoon, I.A.K.; Lawrence, R.D.; Lillie, R.J. Seismic Data, Geometry, Evolution, and Shortening in the Active Sulaiman Fold-and-Thrust Belt of Pakistan, Southwest of the Himalayas1. *AAPG Bull.* **1994**, *78*, 758–774. [CrossRef]
28. Jadoon, I.A.K.; Ding, L.; Nazir, J.; Idrees, M.; Jadoon, S.-u.-R.K. Structural interpretation of frontal folds and hydrocarbon exploration, western sulaiman fold belt, Pakistan. *Mar. Pet. Geol.* **2020**, *117*, 104380. [CrossRef]
29. Banks, C.J.; Warburton, J. 'Passive-roof' duplex geometry in the frontal structures of the Kirthar and Sulaiman mountain belts, Pakistan. *J. Struct. Geol.* **1986**, *8*, 229–237. [CrossRef]
30. Beck, R.A.; Burbank, D.W.; Sercombe, W.J.; Riley, G.W.; Barndt, J.K.; Berry, J.R.; Afzal, J.; Khan, A.M.; Jurgen, H.; Metje, J. Stratigraphic evidence for an early collision between northwest India and Asia. *Nature* **1995**, *373*, 55–58. [CrossRef]
31. Jadoon, I.; Zaib, M. *Tectonic Map of Sulaiman Fold Belt: 1: 500,000 Scale*; COMSATS University Islamabad (Abbottabad Campus): Abbottabad, Pakistan, 2018.
32. Zhuang, G.; Najman, Y.; Guillot, S.; Roddaz, M.; Antoine, P.-O.; Métais, G.; Carter, A.; Marivaux, L.; Solangi, S.H. Constraints on the collision and the pre-collision tectonic configuration between India and Asia from detrital geochronology, thermochronology, and geochemistry studies in the lower Indus basin, Pakistan. *Earth Planet. Sci. Lett.* **2015**, *432*, 363–373. [CrossRef]
33. Qasim, M.; Tabassum, K.; Ding, L.; Tanoli, J.I.; Awais, M.; Baral, U. Provenance of the Late Cretaceous Pab Formation, Sulaiman fold-thrust belt, Pakistan: Insight from the detrital zircon U–Pb geochronology and sandstone petrography. *Geol. J.* **2022**, *57*, 4439–4450. [CrossRef]
34. Chen, Y.; Ding, L.; Li, Z.; Laskowski, A.K.; Li, J.; Baral, U.; Qasim, M.; Yue, Y. Provenance analysis of Cretaceous peripheral foreland basin in central Tibet: Implications to precise timing on the initial Lhasa-Qiangtang collision. *Tectonophysics* **2020**, *775*, 228311. [CrossRef]
35. Coward, M.P.; Rex, D.C.; Khan, M.A.; Windley, B.F.; Broughton, R.D.; Luff, I.W.; Petterson, M.G.; Pudsey, C.J. Collision tectonics in the NW Himalayas. *Geol. Soc. London Spec. Publ.* **1986**, *19*, 203–219. [CrossRef]
36. Kakar, M.I.; Kerr, A.C.; Mahmood, K.; Collins, A.S.; Khan, M.; McDonald, I. Supra-subduction zone tectonic setting of the Muslim Bagh Ophiolite, northwestern Pakistan: Insights from geochemistry and petrology. *Lithos* **2014**, *202–203*, 190–206. [CrossRef]
37. Barbero, E.; Di Rosa, M.; Pandolfi, L.; Delavari, M.; Dolati, A.; Zaccarini, F.; Saccani, E.; Marroni, M. Deformation history and processes during accretion of seamounts in subduction zones: The example of the Durkan Complex (Makran, SE Iran). *Geosci. Front.* **2023**, *14*, 101522. [CrossRef]
38. Raynolds, R.G.H.; Johnson, G.D. Rate of Neogene depositional and deformational processes, north-west Himalayan foredeep margin, Pakistan. *Geol. Soc. London Memoirs* **1985**, *10*, 297–311. [CrossRef]
39. Quittmeyer, R.C.; Kafka, A.L.; Armbruster, J.G. Focal mechanisms and depths of earthquakes in central Pakistan: A tectonic interpretation. *J. Geophys. Res. Solid Earth* **1984**, *89*, 2459–2470. [CrossRef]
40. Khan, I.H.; Clyde, W.C. Lower Paleogene Tectonostratigraphy of Balochistan: Evidence for Time-Transgressive Late Paleocene-Early Eocene Uplift. *Geosciences* **2013**, *3*, 466–501. [CrossRef]
41. Shah, S. *Stratigraphy of Pakistan: Geological Survey of Pakistan Memoir 22*; GSP: Quetta, Pakistan, 2009.
42. Dickinson, W.R. Interpreting provenance relations from detrital modes of sandstones. In *Provenance of Arenites*; Springer: Berlin/Heidelberg, Germany, 1985; pp. 333–361.

43. Ingersoll, R.V.; Fullard, T.F.; Ford, R.L.; Grimm, J.P.; Pickle, J.D.; Sares, S.W. The effect of grain size on detrital modes; a test of the Gazzi-Dickinson point-counting method. *J. Sediment. Res.* **1984**, *54*, 103–116.
44. Corfu, F.; Hanchar, J.M.; Hoskin, P.W.O.; Kinny, P. Atlas of Zircon Textures. *Rev. Mineral. Geochem.* **2003**, *53*, 469–500. [CrossRef]
45. Rubatto, D. Zircon trace element geochemistry: Partitioning with garnet and the link between U–Pb ages and metamorphism. *Chem. Geol.* **2002**, *184*, 123–138. [CrossRef]
46. Rosa, M.D.; Farina, F.; Marroni, M.; Jeon, H.; Pandolfi, L. U–Pb ages from felsic rocks of the External Ligurian sedimentary mélange (Northern Apennine, Italy): Tracing the pre-Jurassic history of the hyperextended Adria continental margin. *J. Geol. Soc.* **2024**, *181*, jgs2023-2121. [CrossRef]
47. Jackson, S.E.; Pearson, N.J.; Griffin, W.L.; Belousova, E.A. The application of laser ablation-inductively coupled plasma-mass spectrometry to in situ U–Pb zircon geochronology. *Chem. Geol.* **2004**, *211*, 47–69. [CrossRef]
48. Wiedenbeck, M.; Allé, P.; Corfu, F.; Griffin, W.L.; Meier, M.; Oberli, F.; Quadt, A.V.; Roddick, J.C.; Spiegel, W. Three natural zircon standards for u-th-pb, lu-hf, trace element and ree analyses. *Geostand. Newsl.* **1995**, *19*, 1–23. [CrossRef]
49. Ludwig, K.R. User's manual for isoplot 3.00, a geochronlogical toolkit for microsoft excel. *Berkeley Geochronol. Center Spec. Publ.* **2003**, *4*, 25–32.
50. Fornelli, A.; Gallicchio, S.; Micheletti, F.; Langone, A. U–Pb detrital zircon ages from Gorgoglione Flysch sandstones in Southern Apennines (Italy) as provenance indicators. *Geol. Mag.* **2021**, *158*, 859–874. [CrossRef]
51. Myrow, P.; Hughes, N.; Paulsen, T.; Williams, I.; Parcha, S.; Thompson, K.; Bowring, S.; Peng, S.-C.; Ahluwalia, A. Integrated tectonostratigraphic analysis of the Himalaya and implications for its tectonic reconstruction. *Earth Planet. Sci. Lett.* **2003**, *212*, 433–441. [CrossRef]
52. Ravikant, V.; Wu, F.-Y.; Ji, W.-Q. U–Pb age and Hf isotopic constraints of detrital zircons from the Himalayan foreland Subathu sub-basin on the Tertiary palaeogeography of the Himalaya. *Earth Planet. Sci. Lett.* **2011**, *304*, 356–368. [CrossRef]
53. Gehrels, G.; Kapp, P.; DeCelles, P.; Pullen, A.; Blakey, R.; Weislogel, A.; Ding, L.; Guynn, J.; Martin, A.; McQuarrie, N. Detrital zircon geochronology of pre-Tertiary strata in the Tibetan-Himalayan orogen. *Tectonics* **2011**, *30*, TC5016. [CrossRef]
54. Myrow, P.M.; Hughes, N.C.; McKenzie, N.R. Reconstructing the Himalayan margin prior to collision with Asia: Proterozoic and lower Paleozoic geology and its implications for Cenozoic tectonics. *Geol. Soc. London Spec. Publ.* **2019**, *483*, 39–64. [CrossRef]
55. McKenzie, N.R.; Hughes, N.C.; Myrow, P.M.; Banerjee, D.M.; Deb, M.; Planavsky, N.J. New age constraints for the Proterozoic Aravalli–Delhi successions of India and their implications. *Precambrian Res.* **2013**, *238*, 120–128. [CrossRef]
56. DeCelles, P.G.; Gehrels, G.E.; Quade, J.; LaReau, B.; Spurlin, M. Tectonic Implications of U-Pb Zircon Ages of the Himalayan Orogenic Belt in Nepal. *Science* **2000**, *288*, 497–499. [CrossRef] [PubMed]
57. Hu, X.; Wang, J.; BouDagher-Fadel, M.; Garzanti, E.; An, W. New insights into the timing of the India–Asia collision from the Paleogene Quxia and Jialazi formations of the Xigaze forearc basin, South Tibet. *Gondwana Res.* **2015**, *32*, 76–92. [CrossRef]
58. Saylor, J.E.; Sundell, K.E. Quantifying comparison of large detrital geochronology data sets. *Geosphere* **2016**, *12*, 203–220. [CrossRef]
59. Myrow, P.M.; Hughes, N.C.; Derry, L.A.; Ryan McKenzie, N.; Jiang, G.; Webb, A.A.G.; Banerjee, D.M.; Paulsen, T.S.; Singh, B.P. Neogene marine isotopic evolution and the erosion of Lesser Himalayan strata: Implications for Cenozoic tectonic history. *Earth Planet. Sci. Lett.* **2015**, *417*, 142–150. [CrossRef]
60. Roddaz, M.; Said, A.; Guillot, S.; Antoine, P.-O.; Montel, J.-M.; Martin, F.; Darrozes, J. Provenance of Cenozoic sedimentary rocks from the Sulaiman fold and thrust belt, Pakistan: Implications for the palaeogeography of the Indus drainage system. *J. Geol. Soc.* **2011**, *168*, 499–516. [CrossRef]
61. Najman, Y.; Sobel, E.R.; Millar, I.; Luan, X.; Zapata, S.; Garzanti, E.; Parra, M.; Vezzoli, G.; Zhang, P.; Wa Aung, D.; et al. The Timing of Collision Between Asia and the West Burma Terrane, and the Development of the Indo-Burman Ranges. *Tectonics* **2022**, *41*, e2021TC007057. [CrossRef]
62. Qasim, M.; Rehman, Z.U.; Ding, L.; Tanoli, J.I.; Abbas, W.; Jamil, M.; Bhatti, Z.I.; Umar, M. Foreland basin unconformity, Western Himalaya, Pakistan: Timing gap, regional correlation and tectonic implications. *Prog. Earth Planet. Sci.* **2023**, *10*, 51. [CrossRef]
63. Clift, P.; Shimizu, N.; Layne, G.; Blusztajn, J.; Gaedicke, C.; Schlüter, H.-U.; Clark, M.; Amjad, S. Development of the Indus Fan and its significance for the erosional history of the Western Himalaya and Karakoram. *Geol. Soc. Am. Bull.* **2001**, *113*, 1039–1051. [CrossRef]
64. Clift, P.; Shimizu, N.; Layne, G.; Gaedicke, C.; Schlter, H.-U.; Clark, M.; Amjad, S. Fifty-five million years of Tibetan evolution recorded in the Indus Fan. *Eos Trans. Am. Geophys. Union* **2000**, *81*, 277–281. [CrossRef]
65. Li, Q.-H.; Lu, L.; Zhang, K.-J.; Yan, L.-L.; Huangfu, P.; Hui, J.; Ji, C. Late Cretaceous post-orogenic delamination in the western Gangdese arc: Evidence from geochronology, petrology, geochemistry, and Sr–Nd–Hf isotopes of intermediate–acidic igneous rocks. *Lithos* **2022**, *424–425*, 106763. [CrossRef]
66. Zhang, K.-J.; Zhang, Y.-X.; Tang, X.-C.; Xia, B. Late Mesozoic tectonic evolution and growth of the Tibetan plateau prior to the Indo-Asian collision. *Earth-Sci. Rev.* **2012**, *114*, 236–249. [CrossRef]
67. Malkani, M.S.; Mahmood, Z. Revised stratigraphy of Pakistan. *Geol. Surv. Pakistan Record* **2016**, *127*, 1–87.
68. Besse, J.; Courtillot, V. Paleogeographic maps of the continents bordering the Indian Ocean since the Early Jurassic. *J. Geophys. Res. Solid Earth* **1988**, *93*, 11791–11808. [CrossRef]
69. Patriat, P.; Achache, J. India–Eurasia collision chronology has implications for crustal shortening and driving mechanism of plates. *Nature* **1984**, *311*, 615–621. [CrossRef]

70. Treloar, P.J.; Izatt, C.N. Tectonics of the Himalayan collision between the Indian Plate and the Afghan Block: A synthesis. *Geol. Soc. London Spec. Publ.* **1993**, *74*, 69–87. [CrossRef]
71. Umar, M.; Friis, H.; Khan, A.S.; Kelling, G.; Kassi, A.M.; Sabir, M.A.; Farooq, M. Sediment Composition and Provenance of the Pab Formation, Kirthar Fold Belt, Pakistan: Signatures of Hot Spot Volcanism, Source Area Weathering, and Paleogeography on the Western Passive Margin of the Indian Plate During the Late Cretaceous. *Arab. J. Sci. Eng.* **2014**, *39*, 311–324. [CrossRef]